

On the emitting region of X-ray fluorescent lines around Compton-thick AGN

Jiren Liu*

National Astronomical Observatories, 20A Datun Road, Beijing 100012, China

ABSTRACT

X-ray fluorescent lines are unique features of the reflection spectrum of the torus when irradiated by the central AGN. Their intrinsic line width can be used to probe the line-emitting region. Previous studies have focused on the Fe $K\alpha$ line at 6.4 keV, which is the most prominent fluorescent line. These studies, however, are limited by the spectral resolution of currently available instruments, the best of which is $\sim 1860 \text{ km s}^{-1}$ afforded by the *Chandra* High-Energy Grating (HEG). The HEG spectral resolution is improved by a factor of 4 at 1.74 keV, where the Si $K\alpha$ line is located. We measured the FWHM of the Si $K\alpha$ line for Circinus, Mrk 3, and NGC 1068, which are 570 ± 240 , 730 ± 320 , and $320 \pm 280 \text{ km s}^{-1}$, respectively. They are 3 – 5 times smaller than those measured with the Fe $K\alpha$ line previously. It shows that the intrinsic widths of the Fe $K\alpha$ line are most likely to be over-estimated. The measured widths of the Si $K\alpha$ line put the line-emitting region outside the dust sublimation radius in these galaxies. It indicates that for Compton-thick AGN, the X-ray fluorescence material are likely to be the same as the dusty torus emitting in the infrared.

Key words: atomic processes – galaxies: Seyfert – galaxies: individual: (Circinus, Mrk 3, NGC 1068) – X-rays: galaxies

1 INTRODUCTION

The obscuring torus around active galactic nuclei (AGN) is a cornerstone of the unification scheme of AGN. In the traditional model the inclination of the torus to the observer is supposed to be responsible for the major differences between type I and type II AGN (e.g. Antonucci 1993). The location of torus was first considered to be on parsec scale, large enough to obscure the broad line region (BLR) and small enough not to obscure the narrow line region (Krolik & Begelman 1988). This is confirmed by recent infrared interferometric observations of several nearby galaxies (see Netzer 2015, for a recent review). The presence of the obscuring torus is also revealed by the Compton reflection component in the X-ray spectra of AGN, which is characterized by the fluorescent Fe $K\alpha$ line (6.4 keV). The parsec-scale distance of the emitting region of the Fe $K\alpha$ line is evidenced by the stability of the Fe $K\alpha$ line (e.g. Bianchi 2012). The exact location of the emitting region can be estimated based on the intrinsic width of the X-ray fluorescent lines (e.g. Shu et al. 2011, and reference therein).

The measurement of the intrinsic line width, however, is limited by the spectral resolution of currently available instruments. The *Chandra* High Energy Transmission Grating Spectrometer (HETGS, Canizares et al. 2005) provides a best spectral resolution

of 0.012 \AA (full width half maximum, FWHM) with its High Energy Grating (HEG), which at 6.4 keV corresponds to $\sim 1860 \text{ km s}^{-1}$, very close to the measured mean FWHM of the Fe line (2000 km s^{-1}) by Shu et al. (2011). We note that the HEG spectral resolution can be improved for lines at lower energies. Therefore, the measurement of the line width can be improved by using the other fluorescent lines, such as the Si $K\alpha$ line at 1.74 eV, where the HEG spectral resolution is $\sim 500 \text{ km s}^{-1}$, a factor of 4 times better than that at 6.4 keV.

The non-Fe fluorescent lines are generally weak, due to their small yields. Nevertheless, they are still observable, especially for Compton-thick AGN, the intrinsic continua of which are heavily suppressed below 10 keV and the observed spectra are dominated by the reflected component from the torus (e.g. Comastri 2004). For example, a series of $K\alpha$ fluorescent lines of Si, S, Ar, Ca, Cr, and Mn are detected in M51, a low-luminosity Compton-thick AGN (Xu et al. 2016).

In this Letter we compile a sample of Compton-thick AGN observed with *Chandra* HETGS to measure their intrinsic width of the Si $K\alpha$ line and estimate the location of the emitting region of the X-ray fluorescent lines. The errors quoted are for 90% confidence level.

* E-mail: jirenliu@nao.cas.cn

Table 1. List of the Compton-thick AGN observed with *Chandra* HETGS

Name	I(Si K α) 10 ⁻⁶ # cm ⁻² s ⁻¹	σ (Si K α) eV	I(Mg XII Ly β) 10 ⁻⁶ # cm ⁻² s ⁻¹	σ (Mg XII Ly β) eV	M_{BH} M_{\odot}	v_{FWHM} km s ⁻¹	r pc
Circinus	3.7 ± 0.7	1.4 ± 0.6	2.4 ± 0.6	1.3	1.7 × 10 ⁶	570 ± 240	0.03 ^{+0.06} _{-0.015}
Mrk 3	3.2 ± 1.0	1.8 ± 0.8	2.3 ± 0.9	3.4	4.5 × 10 ⁸	730 ± 320	4.9 ^{+9.7} _{-2.7}
NGC 1068	6.4 ± 1.5	0.8 ± 0.7	3.5 ± 1.2	2.0	8.6 × 10 ⁶	320 ± 280	0.5 ^{+3.0} _{-0.36}

Note: I is the fitted line intensity and σ the fitted line width. σ (Mg XII Ly β) is fixed at the value measured from the Mg XII Ly α line. The masses of the black hole (M_{BH}) are quoted from Greenhill et al. (2003), Lodata & Bertin (2003), and Woo & Urry (2002), respectively.

2 OBSERVATIONAL DATA

One complexity of using the Si K α line (1.74 keV) is that it is blended with the Mg XII Ly β line at 1.745 keV (the fluorescent wavelengths are from Bearden 1967, while the other wavelengths are from NIST¹). The peaks of these two lines can be resolved by HEG, provided that the signal is good enough. We searched the *Chandra* data archive for Compton-thick AGN observed with HETGS and found that the data of the Circinus galaxy, Mrk 3, and NGC 1068 can be used to measure the two lines simultaneously. The exposure times are 600, 400, and 400 ks, respectively. We use the data downloaded from *Chandra* Transmission Grating Data Archive and Catalog (TGCat, Huenemoerder et al. 2011). All the spectra are extracted from a region with a 2 arcsec half-width in the cross-dispersion direction. The data from ± 1 order of HEG are combined together. The HEG spectra of all the three sources have been published in the literature, such as Sambruna et al. (2001) and Arévalo et al. (2014) for Circinus galaxy, Sako et al. (2000) for Mrk 3, and Ogle et al. (2003) and Kallman et al. (2014) for NGC 1068.

3 RESULTS

The line complexes around 1.74 keV of Circinus, Mrk 3, and NGC 1068 observed with *Chandra* HEG are plotted in Fig. 1. The data are binned to 0.005 Å with a minimum signal-to-noise ratio of 3.3. As can be seen, the line complexes are dominated by the Si K α line at 1.74 keV, but skewed toward higher energy where the Mg XII Ly β line is located. The peaks of the two lines are resolved for Circinus and NGC 1068, while they are blended for Mrk 3. To check the degrading of the spectral resolution due to the spatial extent of the Si K α line, we extracted the radial profile of the 1.74 keV line complex (with a width of 20 eV) from the zero-order images of the three sources, and found that it is consistent with the instrument PSF profile for all three sources. Therefore, the HEG resolving power is not affected much by the spatial extent of the Si K α line.

We fit the line complex with two Gaussian lines plus a power-law continuum. The shift and width of the Mg XII Ly β line are fixed with the values measured from the Mg XII Ly α line at 1.472 keV. Since the Mg XII Ly α and Ly β lines are from the same ions, their line properties should be the same. The fitting region is between 1.5 and 2.3 keV by neglecting the other main emission features. The fitted results are plotted in Fig. 1 and listed in Table 1.

From Fig. 1 we see that the line complexes around 1.74 keV are reasonably fitted by the adopted model. The residuals around 1.73 keV are likely due to the Al XIII Ly α line, while those above

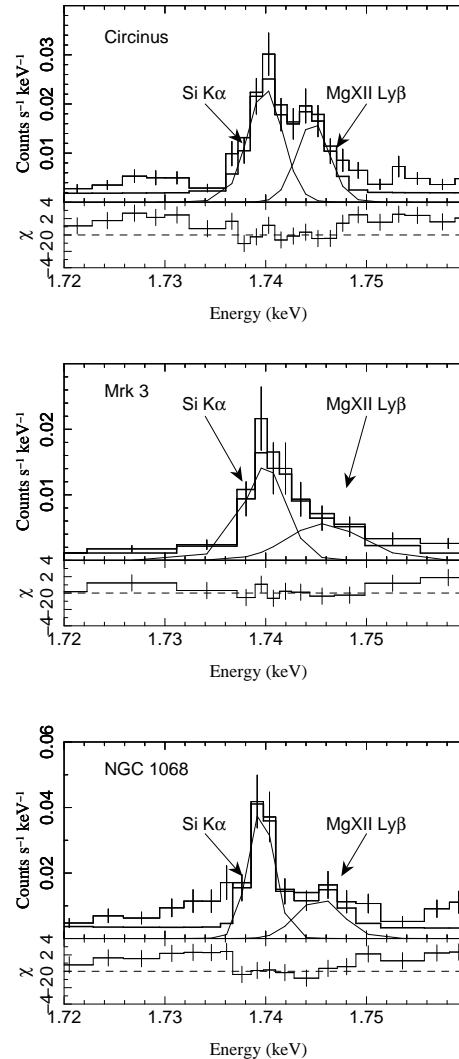


Figure 1. The *Chandra* HEG spectra of the Si K α and Mg XII Ly β line complex of Circinus, Mrk 3, and NGC 1068, corrected for redshift. The fitted models of two Gaussian lines plus a power-law continuum are plotted as the thick solid lines, while the thin lines indicate individual components.

1.75 keV are likely due to the fluorescent lines from singly ionized Si⁺ (1.753 keV, Bearden 1967), the fluxes of which are much smaller compared with those from neutral Si. The fitted line widths of the Si K α line are 1.4 ± 0.6 , 1.8 ± 0.8 , and 0.8 ± 0.7 eV, for Circinus, Mrk 3, and NGC 1068, respectively. They correspond to FWHM velocities (v_{FWHM}) of 570 ± 240 , 730 ± 320 , and 320 ± 280 km s⁻¹. Assuming the line-emitting material is in a virialized orbit

¹ www.nist.gov/pml

around the black hole, its distance to the black hole can be estimated as (Netzer 1990) $r = 4c^2/3v_{\text{FWHM}}^2 r_g$, where $r_g = GM_{\text{BH}}/c^2$. Adopting the black hole masses listed in Table 1, the distances of the line-emitting region are 0.03 pc, 4.9 pc, and 0.5 pc, for Circinus, Mrk 3, and NGC 1068, respectively. We note that the numerical factor 4/3 in the above formula suffers from the uncertainty of the geometrical and dynamical assumptions of the line-emitting material. For example, if it is in a shape of thick disk with $h/r < 1$, the factor becomes $4(h^2/r^2 + \sin^2 i)$, where i is the inclination to the line of sight (Netzer 2013). On the other hand, if the line-emitting material is in some kind of outflow, the factor will depend on the dynamical modelling of the flow.

4 CONCLUSION AND DISCUSSION

X-ray fluorescent lines are unique features of the reflection spectrum emitted by the torus when irradiated by the central AGN. They are most prominent for Compton-thick sources, the intrinsic spectra of which are hidden from direct viewing. The intrinsic line width of the X-ray fluorescent lines can be used to probe the location of the line-emitting region. Using the Si $K\alpha$ line at 1.74 keV, for which the *Chandra* HEG has a spectral resolution ~ 4 times better than for the Fe $K\alpha$ line at 6.4 keV, we measured the FWHM of the Si $K\alpha$ line for Circinus, Mrk 3, and NGC 1068. They have a FWHM of 570, 730, 320 km s⁻¹, respectively. These values are 3–5 times smaller than those measured with the Fe $K\alpha$ line, which are 1710, 3140, and 2660 km s⁻¹, respectively (Shu et al. 2011).

While the ionization potentials of the valence electrons of neutral Si and Fe are similar, the ionization potential of the K-shell electrons of Fe is larger than that of Si. Since the hard photons can penetrate deeper into the material, in principle, the emitting region of the Fe $K\alpha$ line should not be smaller than that of the Si $K\alpha$ line. Therefore the intrinsic line widths of the Fe $K\alpha$ line should not be larger than those of the Si $K\alpha$ line, and they are most likely to be over-estimated. While the limited spectral resolution is likely to be a major reason for the over-estimation, there are several other reasons that could lead to a large measured width of the Fe $K\alpha$ line.

First, the neutral Fe $K\alpha$ line is composed of a doublet, $K\alpha_1$ at 6.404 keV, and $K\alpha_2$ at 6.391 keV, with a flux ratio of 2:1 (Bearden 1967). This leads to a difference of 13 eV (610 km s⁻¹), which is comparable to the FWHM of HEG at 6.4 keV. Secondly, the observed Fe $K\alpha$ line may not come only from the neutral Fe, and is likely blended with those from other low-ionized Fe ions, the energies of which are higher than 6.4 keV by tens of eV (Kaastra & Mewe 1993). Thirdly, the Compton scattering of the Fe $K\alpha$ photons also tends to enlarge the width of the Fe $K\alpha$ line. These intrinsic spreading makes the measurement of the intrinsic line width of the Fe $K\alpha$ line difficult even with instruments of higher spectral resolution. Therefore one should be cautious when using the measured width of the Fe $K\alpha$ line to infer the line-emitting region.

The Si $K\alpha$ line is also composed of a doublet (at 1.7400 keV and 1.7394 keV) with a difference of 0.6 eV (100 km s⁻¹), which is well below the HEG spectral resolution. As the Si $K\alpha$ line is well resolved from the singly ionized Si⁺ $K\alpha$ line (1.753 keV), it represents the truly cold torus, different from the Fe $K\alpha$ line, which may be contaminated by ionized Fe ions. It is interesting to compare the estimated distances of the line-emitting region with the dust sublimation radius r_{dust} . Using the scaling relation obtained from the reverberation measurements of the inner dust radius by Koshida et al. (2014), the r_{dust} are 0.02, 0.15, and 0.11

pc for Circinus, Mrk 3, and NGC 1068, respectively. Therefore, the estimated line-emitting regions are located outside the r_{dust} . This is in contrast to the recent claims that the line-emitting regions are within the r_{dust} based on the measured width of the Fe $K\alpha$ line (e.g. Minezaki & Matsushita 2015; Gandhi et al. 2015). The line-emitting distances estimated from the width of Si $K\alpha$ line are also consistent with the recent infrared interferometric observation of Circinus on sub-parsec scale (Tristram et al. 2014) and NGC 1068 on parsec scale (López-Gonzaga et al. 2014). It shows that for Compton-thick AGN, the X-ray fluorescence material are likely to be the same as the dusty torus emitting in the infrared.

The samples we studied only include 3 galaxies. There are other several galaxies, for which the Si $K\alpha$ lines are detected significantly, although the existing data are not deep enough to allow a deblending of the Mg XII Ly β line yet, such as NGC 4507 and NGC 7582. With further observations of moderate exposure times (200 – 300 ks), the kind of studies conducted here can also be applied to these samples. Beside the Si $K\alpha$ line, the fluorescent $K\alpha$ lines of S, Ar, and Ca are also detected for all three sources, but with a lower S/N due to the quick decline of the effective area of HEG above 2 keV. The signals are generally too weak to provide useful constraints on the line width. Nevertheless, the effective area around these lines will be improved with the forthcoming soft X-ray calorimeter on-board Astro-H, which has a spectral resolution ~ 7 eV.

Because the Si $K\alpha$ line is more sensitive to the absorption than the Fe $K\alpha$ line, the flux ratio between the Fe $K\alpha$ line and Si $K\alpha$ line will be a useful probe of the torus. For example, if the torus is clumpy, the Si $K\alpha$ line will not be significantly reduced, due to its pass through the free-of-obscurations regions between the clumps (e.g. Nandra & George 1994; Liu & Li 2014). Unlike the measurement of the line widths presented here, which needs deep data to resolve the Mg XII Ly β line, the Fe $K\alpha$ /Si $K\alpha$ ratio can be calculated for a larger sample with less S/N. We have compared the Fe $K\alpha$ /Si $K\alpha$ ratio of 10 type II AGN with the simulation of clumpy torus (Liu & Li 2014), and found that the clumpy torus is preferred. The detailed results are presented in Liu et al. (2016). These results show that non-Fe fluorescent lines at soft X-ray band are a potential powerful probe of the torus around AGN.

ACKNOWLEDGEMENTS

We thank our referee for constructive suggestions and Liu Yuan for valuable comments on an early draft. JL is supported by NSFC grant 11203032. This research is based on data obtained from the *Chandra* Data Archive.

REFERENCES

- Antonucci, R. 1993, *ARA&A*, 31, 473
- Arévalo, P., Bauer, F. E., Puccetti, S., et al. 2014, *ApJ*, 791, 81
- Bearden J. A. 1967, *Rev. Mod. Phys.*, 39, 78
- Bianchi, S., Maiolino, R., Risaliti, G. 2012, *AdAst*, 2012, 782030
- Canizares, C. R., Davis, J. E., Dewey, D., et al. 2005, *PASP*, 117, 1144
- Comastri, A. 2004, *ASSL*, 308, 245
- Gandhi, P., Hönig, S. F., Kishimoto, M. 2015, *ApJ*, 812, 113
- Greenhill, L. J., Booth, R. S., Ellingsen, S. P., Herrnstein, J. R., Jauncey, D. L., McCulloch, P. M., Moran, J. M., Norris, R. P., Reynolds, J. E., Tzioumis, A. K. 2003, *ApJ*, 590, 162

- Huenemoerder, D. P., Mitschang, A., Dewey, D., et al. 2011, *AJ*, 141, 129
- Kallman, T., Evans, D. A., Marshall, H., Canizares, C., Longinotti, A., Nowak, M., Schulz, N. 2014, *ApJ*, 780, 121
- Kaastra, J. S. & Mewe, R. 1993, *A&AS*, 97, 443
- Krolik, J. H. & Begelman, M. C. 1988, *ApJ*, 329, 702
- Koshida, S., Minezaki, T., Yoshii, Y., Kobayashi, Y., Sakata, Y., Sugawara, S., Enya, K., Suganuma, M. 2014, *ApJ*, 788, 159
- Liu, Y. & Li, X. 2014, *ApJ*, 787, 52
- Liu, J., Liu, Y., Li, X., Xu, W., Gou, L., Cheng, C. 2016, submitted to *MNRAS*
- Lodato, G. & Bertin, G. 2003, *A&A*, 398, 517
- López-Gonzaga, N.; Jaffe, W.; Burtscher, L.; Tristram, K. R. W.; Meisenheimer, K. 2014, *A&A*, 565, 71
- Minezaki, T. & Matsushita, K. 2015, *ApJ*, 802, 98
- Nandra, K. & George, I. M. 1994, *MNRAS*, 267, 974
- Netzer H. 1990, in Blandford R. D., Netzer H., Woltjer L., eds, *Active Galactic Nuclei*. Springer-Verlag, Berlin, p. 137
- Netzer, H. 2013, *The Physics and Evolution of Active Galactic Nuclei*, Cambridge, UK
- Netzer, H. 2015, *ARA&A*, 53, 365
- Ogle, P. M., Brookings, T., Canizares, C. R., Lee, J. C., Marshall, H. L. 2003, *A&A*, 402, 849O
- Sako, M., Kahn, S. M., Paerels, F., Liedahl, D. A. 2000, *ApJ*, 543, L115
- Sambruna, R. M., Netzer, H., Kaspi, S., Brandt, W. N., Chartas, G., Garmire, G. P., Nousek, J. A., Weaver, K. A. 2001, *ApJ*, 546, L13
- Shu, X. W., Yaqoob, T., Wang, J. X. 2011, *ApJ*, 738, 147
- Tristram, K. R. W.; Burtscher, L.; Jaffe, W.; Meisenheimer, K.; Hönig, S. F.; Kishimoto, M.; Schartmann, M.; Weigelt, G. 2014, *A&A*, 563, 82
- Woo J. H. & Urry C. M. 2002, *ApJ*, 579, 530
- Xu, W., Liu, Z., Gou, L., Liu, J. 2016, *MNRAS*, 455, L26
- Yaqoob, T. 2012, *MNRAS*, 423, 3360